REPORT DOCUMENTATION PAGE

Form Approved
OMB No. 0704-0188

1. REPORT DATE *(DD-MM-YYYY)*	2. REPORT TYPE	3. DATES COVERED *(From - To)*
28-09-2010	Journal Article	

4. TITLE AND SUBTITLE

Magnetohydrodynamic Augmentation of Pulse Detonation Rocket Engines (Preprint)

5a. CONTRACT NUMBER

5b. GRANT NUMBER

5c. PROGRAM ELEMENT NUMBER

6. AUTHOR(S)
Jean-Luc Cambier (AFRL/RZSS)
Christopher F. Zeineh, Lord K. Cole, Timothy Roth, Ann R. Karagozian (UCLA)

5d. PROJECT NUMBER

5f. WORK UNIT NUMBER
23041057

7. PERFORMING ORGANIZATION NAME(S) AND ADDRESS(ES)

University of California, Los Angeles
Dept of Mechanical and Aerospace Eng.
48-121 Engineering IV
420 Westwood Plaza
Los Angeles CA 90095-1597

8. PERFORMING ORGANIZATION REPORT NUMBER

AFRL-RZ-ED-JA-2010-401

9. SPONSORING / MONITORING AGENCY NAME(S) AND ADDRESS(ES)

Air Force Research Laboratory (AFMC)
AFRL/RZS
5 Pollux Drive
Edwards AFB CA 93524-7048

10. SPONSOR/MONITOR'S ACRONYM(S)

11. SPONSOR/MONITOR'S NUMBER(S)
AFRL-RZ-ED-JA-2010-401

12. DISTRIBUTION / AVAILABILITY STATEMENT

Approved for public release; distribution unlimited (PA #10484).

13. SUPPLEMENTARY NOTES
For publication in the Journal of Propulsion and Power.

14. ABSTRACT

Pulse detonation engines (PDEs) are the focus of increasing attention due to their potentially superior performance over constant pressure cycle engines. Yet due to its unsteady chamber pressure, the PDE system will either be over- or under-expanded for the majority of the cycle, with energy being used without maximum gain. Magnetohydrodynamic (MHD) augmentation offers the opportunity to extract energy and apply it to a separate stream where the net thrust can be increased. With MHD augmentation, such as in the Pulse Detonation Rocket-Induced MHD Ejector (PDRIME) concept, energy could be extracted from the high speed portion of the system, e.g., through an MHD generator in the nozzle, and then applied directly to another flow or portion of the flow as a body force. This paper explores flow processes and the potential performance of such propulsion systems via high-resolution numerical simulations. In the PDRIME, at the appropriate point in the PDE cycle, the MHD energy extracted from the nozzle is applied in a separate bypass tube by an MHD accelerator, which acts to accelerate the bypass air and potentially impart an overall net positive thrust to the system. An additional magnetic piston applying energy in the PDE chamber can also act in concert with the PDRIME for separate or additional thrust augmentation. Results show potential performance gains under many flight and operating conditions, but with some challenges associated with achieving these gains, suggesting further analysis and optimization are required.

15. SUBJECT TERMS

16. SECURITY CLASSIFICATION OF:			17. LIMITATION OF ABSTRACT	18. NUMBER OF PAGES	19a. NAME OF RESPONSIBLE PERSON
					Dr. Jean-Luc Cambier
a. REPORT	b. ABSTRACT	c. THIS PAGE	SAR	36	19b. TELEPHONE NUMBER *(include area code)*
Unclassified	**Unclassified**	**Unclassified**			N/A

Magnetohydrodynamic Augmentation of Pulse Detonation Rocket Engines
(Preprint)

Christopher F. Zeineh, Lord K. Cole, Timothy Roth, and Ann R. Karagozian

Department of Mechanical and Aerospace Engineering

University of California, Los Angeles

Jean-Luc Cambier

Air Force Research Laboratory, Aerophysics Branch

Edwards AFB, CA 93524

Corresponding Author:
Professor Ann R. Karagozian
Department of Mechanical and Aerospace Engineering
46-147K Engineering IV, UCLA
Los Angeles, CA 90095-1597 USA
Phone: (310) 825-5653; FAX: (801) 697-7370
E-mail: ark@seas.ucla.edu

Submitted for publication in
Journal of Propulsion and Power
September, 2010

Magnetohydrodynamic Augmentation of Pulse Detonation Rocket Engines

Christopher F. Zeineh,* Lord K. Cole,* Timothy Roth,† and Ann R. Karagozian‡

Department of Mechanical and Aerospace Engineering, UCLA, Los Angeles, CA 90095-1597

Jean-Luc Cambier§

Air Force Research Laboratory, Aerophysics Branch, Edwards AFB, CA 93524

Pulse detonation engines (PDEs) are the focus of increasing attention due to their potentially superior performance over constant pressure cycle engines. Yet due to its unsteady chamber pressure, the PDE system will either be over- or under-expanded for the majority of the cycle, with energy being used without maximum gain. Magnetohydrodynamic (MHD) augmentation offers the opportunity to extract energy and apply it to a separate stream where the net thrust can be increased. With MHD augmentation, such as in the Pulse Detonation Rocket-Induced MHD Ejector (PDRIME) concept, energy could be extracted from the high speed portion of the system, e.g., through an MHD generator in the nozzle, and then applied directly to another flow or portion of the flow as a body force. This paper explores flow processes and the potential performance of such propulsion systems via high-resolution numerical simulations. In the PDRIME, at the appropriate point in the PDE cycle, the MHD energy extracted from the nozzle is applied in a separate bypass tube by an MHD accelerator, which acts to accelerate the bypass air and potentially impart an overall net positive thrust to the system. An additional magnetic piston applying energy in the PDE chamber can also act in concert with the PDRIME for separate or additional thrust augmentation. Results show potential performance gains under many flight and operating conditions, but with some

*Graduate Student Researcher

†Graduate Student Researcher; currently Member of the Technical Staff, Northrop-Grumman Electronic Systems

‡Professor, AIAA Fellow; corresponding author (ark@seas.ucla.edu)

§Senior Scientist, AFRL/RZSA.

challenges associated with achieving these gains, suggesting further analysis and optimization are required.

Nomenclature

A	Cross-sectional area
$\vec{B}$	Magnetic field
c	Speed of sound
$\vec{E}$	Electric field
E	Energy
F_L	Lorentz force
R_m	Magnetic Reynolds number
I	Impulse
$\vec{J}$	Current density
K_y	Loading factor
$\dot{m}$	Mass flux
p	Pressure
T	Thrust
u	Velocity
x, y, z	Streamwise, transverse, and axial coordinates
γ	Ratio of specific heats
ρ	Density
σ	Electrical conductivity

Superscript

$*$	Throat value

Subscript

0	Initial value
byp	Bypass
conv	Converging section
div	Diverging section
cham	Chamber value
e	Exit value
open	Open area downstream of nozzle exit
uwall	Upper wall downstream of nozzle exit

I. Introduction

Robust propulsion systems for advanced high speed air breathing and rocket vehicles are critical to the future of military missions, including those for global/responsive strike and assured access to space. A novel combined cycle propulsive concept, the Pulse Detonation Rocket-Induced MHD Ejector (PDRIME) proposed by Cambier,[1] is one of a number of alternative magneto-hydrodynamic (MHD) thrust augmentation ideas that could have promise for application to a wide range of advanced propulsion systems. Taking advantage of the periodic engine cycle associated with the pulse detonation rocket engine (PDRE), the PDRIME involves periodic temporal energy bypass to a seeded airstream, with MHD acceleration of the airstream for thrust enhancement and control. The range of alternative MHD-augmented propulsion configurations that could be employed suggests that the PDRIME type of concept could be applied to supersonic or hypersonic air-breathing systems, space power production for remote sensing systems, and other potential military systems for the mid-to-far term. This paper explores the fundamental flow processes associated with the PDRIME and modifications thereof via numerical simulation.

A. Background: Conventional Rocket Systems and PDREs

Liquid rocket engines typically employ a constant pressure reaction, where reactants are continually fed at high pressure into the combustion chamber and a nozzle expands and exhausts the flow, generating thrust for the vehicle. The general expression for the force or thrust acting on an object takes the form:

$$\mathbf{F}_{body} = \frac{\partial}{\partial t} \iiint_V \rho \mathbf{V} \, dV + \iint_S (\rho \mathbf{V} \cdot \mathbf{dS}) \mathbf{V} + \iint_S p \, \mathbf{dS} \tag{1}$$

where ρ is the local density, $\mathbf{V}$ is the local velocity vector, and $\mathbf{F}_{body}$ is the sum of the thrust and any forces acting from outside the control volume over which the integrals are calculated; in the case of the present studies, F_{body} includes MHD forces. The control volume can be constructed either around the rocket's interior walls or around the nozzle exit, encapsulating all fluid therein. The former method calculates MHD forces as body forces, while the latter calculates the changes in momentum resulting from these forces. Both methods, which we call the pressure flux and momentum flux methods, produce the same results except for a time-delay,[2] and we choose to utilize the pressure in the present study. For a rocket engine with a solid back wall, Equation (1) reduces to the standard expression for rocket thrust:

$$\mathbf{T} = \dot{m} V_e + (p_e - p_a) A_e \tag{2}$$

where $\dot{m}$ is the mass flux of gas exiting the nozzle, V_e is the exhaust velocity, A_e is the

nozzle exit cross-sectional area, p_a is the ambient pressure, and p_e is the pressure at the exit plane of the nozzle. The total impulse I over the course of an engine cycle is calculated by integrating thrust over time t. The maximum thrust[3] for an engine occurs when the exhaust gases are expanded to the point where the pressure at the exit of the nozzle is equal to the ambient pressure in Equation (2). Further expansion of the gas in the nozzle will reduce the thrust, as the ambient pressure will then exceed the exhaust pressure, creating pressure drag. This added drag can outweigh momentum gains arising from the further acceleration of the flow from the nozzle, i.e., the increase in exhaust velocity. Under-expansion in the nozzle will result in lower than optimal thrust as the maximum momentum gains are not realized. MHD augmentation is in part designed to control the exhaust pressure.

One alternative and theoretically more efficient configuration to the traditional rocket engine is the pulse detonation engine or PDE, a subset of which is the pulse detonation rocket engine or PDRE. The pulse detonation engine operates in a cycle wherein reactants are mixed into the combustion chamber at low pressure, the mixture is ignited, and a detonation wave propagates across the chamber, raising the pressure and temperature and creating a constant volume reaction, which is more efficient than a constant pressure reaction.[4] After the detonation wave (or shock wave, after reactants have been consumed) exits the nozzle, a reflected expansion wave propagates into the chamber, lowering the overall pressure throughout the chamber, and upon reflection at the thrust wall allows reactants to be drawn into the chamber. The reflection of the expansion wave at the nozzle exit results in a compression wave, which can be strengthened to become a shock, igniting reactants in the chamber as a detonation and starting the process once again. A number of recent studies have explored the reactive flow and performance characteristics of PDEs of various geometries.[4–8] The PDE was recently tested for the first time in flight on a Scaled Composites Long EZ aircraft,[9] with four PDE tubes operating at a cycle frequency of 20 Hz.

In the past, our group at UCLA[10,11] has explored the influence of PDE geometry, reaction kinetics, and flow processes using high order numerical methods. A fifth-order WENO (weighted essentially non-oscillatory) scheme[12,13] is used for spatial integration of the reactive Euler equations, with a third -order Runge-Kutta time integration in the case of simplified reaction kinetics; a stiff ODE solver was used for temporal integration in complex kinetics simulations. While the simulations using complex kinetics provide useful quantitative data, the simulations with reduced kinetics (a single step reaction) in fact can provide very similar quantitative performance results.

In general, two different methods could be used to generate thrust for the PDRE. The first involves a straight or slightly contoured nozzle as examined for the PDE. The main goal of this configuration is to exploit the thrust generation from the reflection of the wave, the ignition of the detonation near the thrust wall, and its propagation through the device, as

described above. The second approach is more similar to a constant-pressure rocket. Here the nozzle throat area A_t is very small, small enough to prevent the main detonation wave fom escaping the chamber. This creates multiple reflected compressive waves in the chamber which homogenize the chamber pressurization, resulting in an approximately constant volume reaction. During the blowdown period the reactants are driven out from the chamber and through the nozzle. Similar to the constant-pressure rocket, the exhaust gases are expanded, increasing the velocity and reducing the pressure. The difference between this type of PDRE and a constant-pressure rocket is that in the PDRE, the chamber pressure is decreasing throughout the blowdown period as mass is ejected from the chamber, with no immediate replacement. New reactants are added to the combustion chamber once the pressure has been reduced to a specified value and then the cycle is repeated.

Due to the unsteady nature of the chamber pressure, however, a PDRE nozzle can only be perfectly expanded briefly within a blowdown period. This implies suboptimal use of energy to attain this condition for most of the cycle. At low altitudes, nozzles with large area ratios are subject to large drag forces ($p_a > p_e$ in Equation (2)), while nozzles with relatively smaller exit areas will be under-expanded for the majority of blowdown. Whether or not the configuration includes a converging section, the lack of perfect matching conditions essentially negates the benefits of a constant-volume combustion.[14]

B. The PDRIME Concept

Ejectors are often used to transfer energy from one stream to another stream, providing an additional source of thrust, especially for an air-breathing engine. Ejectors have been shown to produce overall thrust gains when energy is taken from a high velocity flow and transferred to a low energy stream (in the ejector) that has a high mass flow rate. In the present application for the PDRE, energy can be extracted from the nozzle when the marginal decreases in thrust are small and added to a bypass air flow which acts as an ejector to assist in augmentation of the thrust. Ejectors typically transfer energy between streams through shear stress between separate flow streams, where a portion of the main flow is diverted into a channel to mix with the lower velocity flow. The drawback of this method is that the ability to transfer energy is limited by the contact area and the slow rate of viscous transport between the two streams. At large velocities, shear layer thicknesses are small, leading to the necessity for large channels and/or large interfacial surfaces such as lobed shapes[15] for mixing, which add weight to the vehicle.

In contrast, if magnetohydrodynamic (MHD) forces are applied as body forces to the ejector flow, affecting the entire flow field immediately, there can be benefits. This could reduce the length of the bypass tube and time necessary for complete energy transfer as well as providing the flexibility of energy extraction and application, since the applied fields

can be varied.[16] One possible configuration attaches a converging-diverging nozzle to the combustion chamber of a PDRE with a bypass tube. Just as the AJAX concept proposes to divert energy from an inlet flow by an MHD generator before reapplying it after the combustor via an MHD accelerator, this energy bypass concept could also be applied to the PDRE.[16]

A generic configuration for this concept, the Pulse Detonation Rocket Induced MHD Ejector (PRDIME), is shown in Figures 1a and 1b, where the interaction between a magnetic field and an electrically conducting fluid flow (MHD) takes place. For the present applications, magnetic and electric fields are applied both normal to each other, in the z and y directions, respectively, and normal to the fluid velocities (which are, in the nozzle and bypass-tube, in the x-direction). In the expanding (divergent) section of the nozzle, magnetic and electric fields are applied to extract energy from this portion of the flow. A bypass-tube sits adjacent to the engine. Ambient air enters this tube and is accelerated by an MHD accelerator powered by the energy extracted from the nozzle. A gain in thrust is realized by extracting energy from the nozzle, which would otherwise be used inefficiently, and by applying the energy to the air in the bypass-tube. A planar design is used here to achieve a spatially uniform magnetic field, only in the z-direction, by placement of magnets above and below each region.

The evolution of the flow cycle for the PDRIME is shown in Figures 1a and 1b. Because a PDRE can be designed to have a converging-diverging nozzle such that the initial peak pressure in the combustion chamber results in pressure at the nozzle exit plane that is well above ambient, a contact surface originates at the nozzle lip and extends to the upper wall of the bypass tube, creating conditions for an unsteady shock with propagates into the bypass channel, as shown in Figure 1a. If the air in the bypass channel is initially at high Mach number, this traveling shock brings the air to a high temperature. If a species such as cesium can be added to the flow, high conductivity can be attained by thermal ionization. Hence the shock generates a slowly-moving slug of high-temperature air, shown as the shaded section in Figure 1a, that can be more easily ionized. This approach eliminates the need for non-equilibrium ionization, as in the AJAX concept.

As the pressure at the nozzle exit drops during blowdown, the shock then slows down, and eventually the ionized air in the bypass section starts to move downstream. At this point, electrical power can be applied via an MHD accelerator to eject the air slug from the bypass tube and thus generating thrust (Figure 1b). The procedure can then be repeated at each cycle. One only needs to design the nozzle such that the flow is under-expanded during the initial part of the blowdown phase. In fact, there may be a self-adjusting process at work, depending on PDRE nozzle design and altitude as outlined by Cambier.[14] While at launch, the nozzle exit pressure is equal to ambient and there is no interaction with the

bypass air, as the vehicle accelerates and gains altitude, the nozzle becomes progressively under-expanded, so that eventually a strong shock can be generated for the bypass channel to ionize the seeded air, and the ejector operates. This is one of several configurations in which the PDRIME concept could be used for thrust augmentation in advanced propulsion systems.

As noted above, the MHD generator is located in the diverging section of the nozzle where the velocity is largest, so that the expansion of the fluid counteracts some of the velocity reduction arising from the Lorentz (drag) force acting in the generator. The Lorentz force acts on all conductors carrying a current of density $\vec{J}$ in a magnetic field of strength $\vec{B}$. This force is given in general by:

$$\vec{F}_L = \vec{J} \times \vec{B} \tag{3a}$$

or, for the orientation of vectors in Figure 1:

$$\vec{F}_{L,x} = \vec{J}_y \times \vec{B}_z \tag{3b}$$

The current density $\vec{J}$ is an important property of the MHD flow system which is related to electric and magnetic fields, $\vec{B}$ and $\vec{E}$ respectively, and the velocity vector $\vec{u}$ via Ohm's law:

$$\vec{J} = \sigma(\vec{E} + \vec{u} \times \vec{B}) \tag{4}$$

where σ is the electrical conductivity (with units of Mho/m). For the PDRIME orientation described in Figure 1, this reduces to a current density with a component in the y-direction only:

$$J_y = \sigma(E_y - u_x B_z) \tag{5}$$

where $\vec{E}_y$ is the electric field acting in the y-direction and $\vec{B}_z$ is the magnetic field acting in the z-direction. A magnetic Reynolds number, R_m, is a dimensionless parameter which indicates the magnitude of these interactions:

$$R_m = \mu\sigma u L \tag{6}$$

where μ is the permeability of free space (units of N/A^2), u is the velocity magnitude and L is a characteristic length scale. The motion of the electrically conducting fluid induces an additional magnetic field, but for low magnetic Reynolds numbers, this is negligible and the magnetic field may be considered constant. A low magnetic Reynolds number approximation is assumed for our MHD applications.

Note that with a constant and positive magnetic field, the direction of the current density and thus of the Lorentz force depends on the relative magnitudes of E_y and $u_x \times B_z$ from Equation (5). We define a loading factor, K_y, to compare these strengths:

$$K_y = \frac{E_y}{u_x B_z} \tag{7}$$

When $|K_y|$ is less than unity, the current density in the y-direction is negative, resulting in a Lorentz force opposing the fluid motion. Energy effects of MHD application are governed by the current density multiplied by the electric field. This energy source term can be decomposed as follows:

$$\vec{J} \cdot \vec{E} = \frac{\vec{J}^2}{\sigma} + \vec{u} \cdot (\vec{J} \times \vec{B}) \tag{8}$$

where the terms on the right hand side represent the dissipative heating and mechanical power, respectively. When the magnitude of the loading factor $|K_y|$ is less than 1, the mechanical power is negative because energy is being extracted from the fluid. Thus in the PDRIME configuration, for MHD generation in the nozzle, the loading factor is greater than 0 and less than 1, causing energy to be extracted from the fluid in the nozzle with a negative Lorentz force. In the accelerator (bypass section), a positive Lorentz force and application of energy takes place (Figure 1a), with $|K_y| > 1$. Regardless of the loading factor, the ohmic heating will always be a positive term, representing a loss in both cases. Ignoring dissipative effects, we see that the Lorentz force scales with velocity, while the energy associated with both generation and acceleration scales with velocity squared. For this reason, maximum thrust gain is achieved when energy is extracted from high velocity flows, as in the nozzle, and applied to low velocity flows.[16]

The optimal loading factor magnitude $|K_y|$ for MHD generation is shown to be 0.5. For $|K_y| < 1$, the goal is to extract maximum power (K_y) with minimal dissipation (K_y^2). The energy generated in the nozzle is then applied in the bypass-tube by an MHD accelerator. Under all circumstances, if the loading factor in the bypass tube is greater than unity, we choose $|K_y| = 1.5$, in order to accelerate the flow. But if a negative flow is detected in that location in the course of the cycle, $|K_y| = 0.5$ is assumed in the present study in order to help decelerate it.

C. The Magnetic Piston Concept

Another alternative configuration by which MHD can be used to augment thrust generated by a PDRE is one in which energy extracted by MHD from the high velocity flow in the expansion portion of the nozzle can be applied to the combustion chamber in order to accelerate combustion products from the chamber while allowing a fresh mixture of reactants

to fill the available volume. Creation of this magnetic piston in the chamber, as outlined in Cambier,[14] can be used to push combustion products from the chamber while allowing a fresh mixture of reactants to fill the available volume. Such a configuration is shown in Figure 2. As noted above, extraction of energy from a high velocity stream and delivered to a low velocity stream is one mechanism for thrust augmentation, hence a configuration such as that in Figure 2 can theoretically lead to performance gains. As indicated by Cambier,[14] thrust increases with an increasing fraction of energy extracted from the flow, and with reduction in the filling time. When blowdown and filling processes are allowed to overlap via appropriate application of the magnetic field, filling time is effectively reduced, leading to a large increase in average thrust. The magnetic piston concept, separately as well as in concert with the PDRIME with bypass flow, will be explored here.

The goal of the present research involves use of a simplified model for the blowdown portion of the PDRE, coupled to a more detailed simulation of the relevant MHD processes in the nozzle and/or adjacent bypass sections, as a means of predicting overall PDRIME and magnetic piston phenomena and performance parameters. The model has been validated using detailed numerical simulations of PDRE processes,[2,11] so that projections for optimal performance and operating conditions may be made.

II. Description of the PDRIME Model and Simulation Procedure

A. Framework and Blowdown Model

Due to the large number of available system parameters in the PDRIME, a rapid simulation technique is required, one that is simpler than a detailed numerical simulation of flow and reactive processes in the PDRE and adjacent flow sections. Resolution of detonations constitutes a major computational cost; the sharp gradients and large sound speeds present in the PDE greatly reduce the time-step and require finer spatial resolution.[17,18] For the PDRE configuration, after the shock waves have subsided in the chamber, the properties of the fluid within the combustion chamber are mostly uniform, resembling the products of a constant volume reaction. For these reasons a blowdown model was developed by Cambier[19] to predict chamber properties as a function of time after a constant volume reaction.

Intuitively, a small throat also restricts the mass flow of propellants out of the chamber, which leads to a slow decay of chamber pressure, increasing the blowdown period.

Cambier's model utilizes a single computational cell to represent a combustion chamber filled with post-constant volume reaction products at high pressure and temperature. The converging section of the nozzle is also represented by a single cell approximation. An

adiabatic solution for the throat conditions for every time-step is determined based on the combustion chamber properties and the assumption that the throat is choked. The divergent section, throat to exit, is fully discretized to account for the MHD coupling, as is the entire bypass-tube. In order to validate certain aspects of the engine cycle and flow processes, comparisons between the blowdown model and full 2D transient numerical simulations are made.

The blowdown evolutions of the stagnation variables in the chamber are calculated as functions of specific heat ratio and time:[14]

$$p_0 = \hat{p}_0[f(t)]^{\frac{\gamma}{\gamma-1}} \tag{9a}$$

$$\rho_0 = \hat{\rho}_0[f(t)]^{\frac{1}{\gamma-1}} \tag{9b}$$

$$T_0 = \hat{T}_0[f(t)] \tag{9c}$$

where the caret ($\hat{}$) indicates the peak value at the start of the blowdown, and the subscript ($_0$) indicates chamber stagnation conditions. The function $f(t)$ as an analytic solution takes the form:

$$f(t) = \frac{1}{(1+\nu t)^2} \tag{10a}$$

where

$$\nu = \frac{(\gamma-1)\Gamma c_0}{2L_{cham}} \frac{A^*}{A_{cham}} \tag{10b}$$

and

$$\Gamma = (\frac{2}{\gamma+1})^{\frac{\gamma+1}{2(\gamma-1)}} \tag{10c}$$

and where t is time, c_0 is the chamber fluid's speed of sound, γ is the specific heat ratio, L_{cham} is the chamber length, A^* is the cross-sectional area at the nozzle throat, and A_{cham} is the cross-sectional area of the chamber. γ and Γ are updated with each time step as new chamber properties are calculated. In this approach the entire combustion chamber is represented with a single cell, greatly reducing computational time.

B. Discretization of Nozzle and Bypass Sections

The diverging section of the nozzle and the bypass-tube are divided into cells. The 2D transient equations which govern this flow in conservative form are similar to those in He and Karagozian,[10,11] but with additional species terms (to simulate air, water vapor exhaust, cesium atoms, and cesium ions), momentum and energy source terms corresponding to MHD

effects, and an ionization/deionization source term when we simulate the injection of cesium:

$$\vec{U}_t + \vec{F}(\vec{U})_x + \vec{G}(\vec{U})_y = \vec{S}(\vec{U}) \tag{11}$$

$$\vec{U} = \begin{pmatrix} \rho \\ \rho u \\ \rho v \\ E \\ \rho Y_{Cs} \\ \rho Y_{Cs^+} \\ \rho Y_{H_2O} \end{pmatrix} \qquad \vec{F}(\vec{U}) = \begin{pmatrix} \rho u \\ \rho u^2 + p \\ \rho uv \\ (E+p)u \\ \rho u Y_{Cs} \\ \rho u Y_{Cs^+} \\ \rho u Y_{H_2O} \end{pmatrix} \tag{12}$$

$$\vec{G}(\vec{U}) = \begin{pmatrix} \rho v \\ \rho uv \\ \rho v^2 + p \\ (E+p)v \\ \rho v Y_{Cs} \\ \rho v Y_{Cs^+} \\ \rho v Y_{H_2O} \end{pmatrix} \qquad S(\vec{U}) = \begin{pmatrix} 0 \\ 0 \\ 0 \\ 0 \\ \dot{\Omega}_{Cs} \\ \dot{\Omega}_{Cs^+} \\ 0 \end{pmatrix} \tag{13}$$

where the total energy term E is given by:

$$E = \frac{p}{\gamma - 1} + \frac{\rho(u^2 + v^2)}{2} + \rho q Y_{Cs^+} \tag{14}$$

where the heat release per unit mass $q = 2.827 \times 10^6 J/k$ (or 375.7 kJ/mol, the first ionization energy of cesium) and is affixed to the mass fraction of cesium ions since ionization is endothermic and no other reactions take place.

Transient flow in the bypass-tube involves a shock created by the nozzle exhaust, traveling into the bypass exit and propagating to the left into a high speed right-moving flow. Quasi-steady forward-marching methods are thus not adequate for these regimes, especially since this method has a singularity when the flow Mach number is equal to one. For these reasons, a fully transient numerical scheme must be used to simulate flow in the bypass-tube.

In simulating flow in the bypass-tube, the WENO method[12] is used to approximate spatial derivatives, with a stencil including upstream and downstream cells. WENO is an adaptation of the Essentially Non-Oscillatory (ENO) method,[13] which uses the conservation laws for high order accuracy with shock capturing capabilities. Artificial viscosity is added via the Local Lax Friedrich (LLF) scheme[10] to avoid entropy violation and reduce dispersion

while introducing dissipation. Temporal integration is performed by a 3rd order Runge-Kutta method, which uses a multistep process to achieve fairly large time-steps without loss of high order accuracy. The time-step is regulated by the Courant-Friedrichs-Levy (CFL) condition, which ensures stability in temporal integration by ensuring that information does not propagate completely through any one computational cell in a given time-step.

C. Geometries and Grid Generation

In quasi-1D simulations of a PDRIME configuration, as described in recent studies,[1,20,21] the computation of quasi-1D flow in the supersonic nozzle flow must be decoupled from that in the bypass tube, with no resolution of the transfer of fluid from the nozzle to the bypass section. These quasi-1D models thus prescribed the bypass exit boundary conditions as a function of the nozzle exit conditions, which themselves are a function of time. The two-dimensional simulations conducted in the present study will explore the full 2D flowfield and will also mimic the conditions under which the quasi-1D tests operated to determine whether the quasi-1D boundary condition functions accurately reflect two-dimensional PDRIME behavior.

In the present study, the 2D configuration for the general form of the planar PDRIME is shown in Figure 3. A_{cham}, A^*, A_e, and A_{byp} are the areas of the chamber, throat, nozzle exit, and bypass, respectively, and L_{cham}, L_{conv}, L_{div}, L_{byp}, L_{uwall}, and L_{open} indicate the lengths of the chamber, converging nozzle, diverging nozzle, bypass tube, upper wall of the bypass extending beyond the nozzle lip, and outflow area from the nozzle lip. The expanding nozzle between the throat and the exit is parabolic so that the curved lip of the nozzle allows shocks to more easily follow the contour of the wall to enter the bypass.

The bypass tube runs straight along the top of the PDE, and although the lower bypass wall ends at the tip of the nozzle, the upper wall can extend further. This extension can help maximize impulse by "catching" the outgoing shock from the nozzle and diverting into the bypass tube to be utilized by the MHD accelerator. The bypass tube should not be excessively wide, or else the shock migrating into the tube ceases to be uniform, creating inefficiencies in the MHD accelerator. It must also not be too narrow, lest not enough fluid become available to accelerate. The geometrical parameters used in the present calculations are given in Table 1.

The grid used for the present two-dimensional calculations consists of a grid of cells measuring n_x cells horizontally by n_y cells vertically, flanked on all four sides by a layer of three ghost cells for spatial interpolation (i.e. boundary conditions) along both axes. The grid for these simulations is shown in Figure 4, representing the PDRIME as well as a downstream area where one can observe the region where the flow from the nozzle into the bypass takes place. Symmetry across the nozzle's centerline enables the 2D grid to simulate

only the upper half of the cross-section of the PDRE, and the centerline is treated as a solid wall boundary. The top of the grid indicates the top of the bypass tube and thus utilizes a reflective boundary condition along the length of the bypass upper wall. An open-air outflow boundary condition is used for the remaining section downstream of the PDRIME. To minimize the thickness of the nozzle wall, we utilize a block grid, in which our larger grid is effectively split into two regions: the nozzle with its exhaust downstream and the bypass with its outflow downstream, as illustrated in Figure 4. This way, the upper nozzle wall and lower bypass wall can meet at a point of zero thickness while the ghost cells needed to simulate either side can be prescribed without hindering each other in a single grid. The nozzle section has as its left boundary condition at the nozzle throat the inlet prescribed by the Cambier blowdown model, as described in Section IIA.

A series of 1D and 2D shock-tube tests conducted by Zeineh[2] allows us determine the minimum resolutions for which the computational grid must be generated. These tests reveal a minimum requirement requirement of 100 cells/meter for the x- and y-axis resolutions. This is the resolution shown in Figure 4 in order to accurately capture shocks being transferred from the nozzle into the bypass section.

D. MHD Application

The MHD generator in the PDRIME configuration should be active only at the divergent section of the nozzle, where it will most benefit performance during the blowdown phase of the cycle. Thus, the generator source terms will be added to the governing equations for only those grid cells lying in the PDRIME between the nozzle throat and the exit, in particular the downstream half of the diverging region where they utilize a loading factor of K_y is 0.5. In the bypass section, the MHD components must act as a generator in places where the average flow travels upstream and as an accelerator when the local flow travels downstream, thus further accelerating the fluid. When acting as a generator, the loading factor K_y is 0.5, and when acting as an accelerator, K_y is 1.5, as noted previously. This can be accomplished by assuming that the capacitors imposing the electric fields are segmented such that they can be independently and simultaneously activated, some as generators and others as accelerators.

A magnetic piston modeled in the chamber operates in the same manner as an MHD accelerator, except that the magnitude of the magnetic field changes in time such that the throat pressure remains constant until the chamber is emptied of products. If we instead model only the diverging nozzle and assign values to the throat inlet based off a blowdown model, we can alternatively use the numerical magnetic piston model to determine its rate of energy consumption while maintaining constant inlet conditions at the throat. Both approaches are explored here.

In all of these cases, the ability of the MHD components to manipulate the flow depends upon the fluid's conductivity, which in turn depends upon the density of cesium ions. Introducing such ions will be accomplished by seeding both the chamber and bypass flows with cesium atoms, which have a low enough ionization energy to be practical for this purpose. The current study simulates the flow of cesium atoms and ions within the PDRIME, calculating conductivity directly, but it also examines an approximation utilized in earlier research by Roth,[1,20] whereby any fluid in the bypass whose temperature exceeds 3000K is assumed to be ionized while any fluid below this threshhold is not. The nozzle flow is under no such restriction since the chamber fluid is assumed to be ionized to equilibrium after the initial detonation has left the PDRE and the convection time scale is much lesss than the chemical time scale, allowing us to assume frozen flow conditions.

III. Results and Performance Evaluation

A. Blowdown Validation

Validity of the blowdown model in representing detonation and shock reflections in a PDRE combustion chamber may be ascertained by comparing the behavior of the modeled blowdown process with actual PDRE blowdown as represented via a detailed, quasi-1D or 2D WENO simulation. The starting conditions of the Cambier model[19] assume that the detonation wave has already left the combustion chamber and that the remaining compression wave has reflected within the chamber sufficiently for the fluid within to become more or less stagant. Since the chamber pressure and temperature in the wake of the repeatedly reflecting compression wave depend directly upon the reactants' pressure and temperature before the detonation, we must establish a set of assumptions to correspond to a set of initial conditions.

For the purposes of this study, we assume the reactants to be a stoichiometric mixture of hydrogen and oxygen, leaving behind pure water vapor in the chamber, and that the water vapor at the start of the blowdown cycle is pressurized to 100 atm and heated to either 3000 K or 4000 K. The fluid in the nozzle is filled with products such that the fluid at the throat is sonic and that the fluid in the converging and diverging sections correspond to a quasi-steady, isentropic compression and expansion. Both quasi-1D and 2D simulations of this blowdown process will be explored in this validation. For two-dimensional simulations, the fluid directly downstream of the nozzle will match the fluid at the nozzle exit, while all fluid outside of the nozzle and above the nozzle exhaust will consist of air at the appropriate altitude. The results will be compared with the ignition and propagation of a detonation and relevant reflection of shocks computed for a quasi-1D PDRE configuration.

The flow and performance characteristics of the quasi-1D PDRE chamber simulation and

the quasi-1D and 2D blowdown model are shown in Figures 5(a) and 5(b). We examine the impulse and chamber pressure using the same base case among the alternative cases. The impulse and pressure plots match up very closely with one another, aside from the fact that we assume the initial flow to be stagnant in the PDRE case. The reflecting shock waves observed in the PDRE chamber also expectedly make the corresponding results less smooth than those from the blowdown method, but any oscillations are also shown to become smooth with time, indicating that our substitution of throat model inlet conditions in place of the combustion chamber is appropriate. On this basis, in order to reduce computational costs in performing PDRIME and other MHD-augmentation concepts, we will utilize Cambier's blowdown model to provide "input" to a detailed simulation of transient flow processes beyond the nozzle throat and, if present, within the PDRIME bypass section.

B. Baseline PDRE with and without Nozzle Generator

The first simulations will utilize the baseline PDRE geometry with only the diverging nozzle and no bypass tube or active MHD components therein. Cambier's blowdown model[19] is utilized for the throat inlet conditions. Initial chamber pressure is set to 100 atm, and simulations will be conducted for the initial chamber temperatures set to both 3000 K and 4000 K. In both cases, we assume that the blowdown phase of the PDRE cycle ends when the chamber pressure reaches 2% of its original value (i.e. 2 atm). When we keep the initial chamber pressure constant but increase the temperature by 1000 K, the impulse per cycle drops from 1150 N-s to 1025 N-s because the initial chamber density has been reduced, thus also reducing the mass available to be expelled from the nozzle.

This calculation is compared with the same PDRE but with the nozzle generator activated, indicated in Figure 6. Quasi-1D, quasi-steady simulations by Roth[20] utilizing the same PDRE design iteratively calculated the magnetic field strength B at each time step such that the nozzle exit Mach number would be 1.2 throughout the blowdown cycle.[14] These data were used to produce a curvefit for the evolution of the magnetic field strength with time that is used in the transient quasi-1D and 2D simulations with the nozzle generator. The generator's domain of operation runs between the midpoint and exit of the diverging nozzle section, and it activates as soon as the blowdown commences. The electrical conductivity σ in this entire region is assumed to hold constant at 1000 Mho/m.

Both the quasi-1D and 2D results for these simulations illustrate how activating the nozzle generator produces energy, but at a cost of reduced impulse due to drag. Figure 6 shows that for a chamber temerature of $T_{0,cham} = 3000K$, the reduction in impulse for the PDRE with the nozzle generator is about 120 N-s at the end of the cycle. About 420 kJ in available energy is generated during this process; this can be used either in the bypass section or in the magnetic chamber piston, as described previously. As expected, calculating impulse

using either the pressure method or momentum flux method produces the similar results; subsequent calculation of impulse use the pressure method. No substantive differences are observed between quasi-1D and 2D results.

The benefits of the nozzle generator in affecting flow from the nozzle to the bypass section may also be explored. The presence of the nozzle generator alone can affect how much of the bypass fluid is blocked by the nozzle exhaust and whether a shock traverses upstream to heat the flow. Figure 7 shows temperature contours for the PDRIME geometry both for the cases without MHD at all and with only the MHD nozzle generator operating for an altitude of 25 km and at flight Mach numbers 7, 9, and 11. This is the altitude and flow regime in which MHD augmentation would have the most benefit according to earlier quasi-1D simulations.[20,21] We observe that much greater heating occurs in the bypass section when we activate the nozzle generator because the higher pressure at the nozzle exit allows a stronger shock, traveling at a higher speed, to enter the bypass section. Increasing the nozzle exit pressure through extraction of the flow's kinetic energy is vital to the heating and ionization of the bypass fluid, which in turn is vital to MHD acceleration for the PDRIME.

Unlike in an idealized quasi-1D simulation of the bypass tube, however, the high-pressure nozzle exhaust does not block the bypass air in such a way that it is brought to a complete halt or even simply decelerates. The contact surface between nozzle exhaust and bypass outflow is not always a vertical wall but lies at an angle that grows more shallow as the Mach number increases.[1] Some air creeps over this contact surface, but the rest circulates back and upstream into the bypass tube, partially inducing numerical mixing with the water vapor from the nozzle and creating exit conditions considerably different from those assumed for quasi-1D PDRIME simulations in earlier research by Roth[20] and Cole.[21]

C. PDRE with Nozzle Generator and Chamber Piston

As noted above, energy generated from the nozzle can be reintroduced within the PDRE's chamber, allowing operation of a magnetic chamber piston. Running the piston and the generator at the same time would be counterproductive, so we activate them in series, where the nozzle generator runs until the chamber pressure reaches a fixed percentage of its initial value (called either the generator shutoff pressure or the chamber activation pressure). Immediately after this point, the magnetic chamber piston utilizes this energy to blow down the remainder of the products. In some cases, not enough energy is available to evacuate all of the remaining products with the piston, in which case normal blowdown resumes after the piston runs out of energy to complete the cycle. Activation pressures that bring about this scenario are said to fall into the "mass-rich" domain. In other cases, the piston is able to evacuate all of the products and still have energy to spare; we call this the "energy-rich" domain. We define the critical pressure to be the activation pressure for which the piston

finishes evacuating the chamber with exactly no energy remaining.

Figure 8 shows the effects of varying the activation pressure on the PDRE with the nozzle generator and magnetic chamber piston operating, in contrast to the same configuration but with zero MHD (no generator or chamber piston operational). Results are shown for the impulse at the end of a cycle (Figure 8(a)) and the amount of energy that can be generated and consumed for different chamber temperatures (Figure 8(b)). The activation pressure at which the energy generated is equal to that consumed by the chamber piston is the critical pressure, which is shown here to be approximately 45 atm.

We note that all of the results for the MHD generator and piston operation shown in Figure 8(a) produce impulse per cycle totals that are below those using no MHD application at all. This is expected for the energy-rich simulations where kinetic energy is extracted from the flow and not completely reallocated (i.e. activation pressure is below the critical pressure), but we also see it in the mass-rich simulations where all available extracted energy is completely reallocated (i.e. activation pressure is greater than the critical pressure). This tells us that while the generator/piston combination can reduce the cycle time and thus possibly improve impulse per unit time at the cost of extra fuel, it does not improve impulse or operative efficiency. Since our goal is to improve efficiency, the piston should be utilized only in conjunction with the bypass accelerator. Ideally, this would mean that energy should not be redirected towards the chamber piston unless the bypass accelerator is unable to utilize all of the energy provided by the generator. If the generator must extract more energy than the bypass accelerator can consume in order to ensure sufficient bypass heating, then the chamber piston can consume the remainder and perhaps be used efficiently. This operation is explored in the PDRIME simulations below.

D. PDRIME Simulations with Constant Conductivity

While the results at flight Mach 7 (Figure 7) produced some heating in the bypass, tests[2] with the 2D PDRIME simulation reveal that not enough of the flow can be maintained at a temperature above 3000 K to facilitate non-negligible MHD acceleration. In contrast, our simulations at Mach 9 and 11 heat up just enough of the bypass fluid to be considered useful, so further 2D simulations with the full PDRIME are conducted only at Mach 9 and Mach 11. Any higher flight speeds at altitudes of 25 km or 30 km cause the heated bypass fluid to be too small to utilize the accelerator. Any slower, and the fluid that is heated will not be hot enough for ionization. First we calculate flow evolution and performance assuming a constant electric conductivity in the flow.

At altitudes of both 25 km and 30 km, and for both flight Mach numbers 9 and 11, the MHD generator heats up the bypass flow enough that the bypass accelerators can reintroduce all available energy into the bypass section at higher activation pressures, meaning that the

chamber piston is not actually needed at times. Results for the total impulse as a function of activation pressure for a chamber temperature of 4000 K, for example, are shown in Figure 9 for different flight Mach numbers and altitudes. In these cases, we activate only the nozzle generator and the bypass accelerator, leaving the chamber piston inactive. The bypass accelerator, however, does not activate until 3.5 ms after the blowdown cycle commences so as to give the nozzle-driven shock sufficient time to propagate and heat the bypass flow. For these simulations in Figure 9, the conductivity in the nozzle is set to 1000 Mho/m, and the conductivity in the bypass is set arbitrarily to 500 Mho/m in regions where the average temperature across a given cross-section exceeds 3000 K; σ is equal to 0 Mho/m elsewhere. The magnetic field strength in the nozzle varies according to the quasi-1D, quasi-steady evolutions determined earlier, while the magnetic field strength in the bypass section is uniformly 3 Tesla. The simulations are for activation pressures of 20 atm, 30 atm, and 40 atm, as these were deemed the most promising from the chamber piston tests for their residing in the energy-rich domain.

What we discover in Figure 9 is that no matter which activation pressure we utilize for the generator, we are never able to produce enough impulse in the bypass to replace the impulse lost by the nozzle generator. Furthermore, the bypass accelerator is able to provide more impulse at an altitude of 25 km than at 30 km, despite the latter case resulting in greater heating of the bypass tube. At both altitudes, worse performance results are observed when more energy is made available to the bypass accelerator, which evidently cannot utilize it as efficiently as it was generated.

These results lie in contrast to those observed in quasi-1D simulations, where at Mach 9 conditions the bypass was able to fully utilize all available energy to positive effect without either shutting off the generator early or activating the chamber piston. Such results are shown, for example, in Figure 10. Comparisons between this quasi-1D simulation and the 2D simulation are difficult due to the varying nature of the MHD component operation (i.e. the 2D results correspond to the nozzle generator being shut off at a chamber pressure of 30 atm, while no such shutoff occurs in the quasi-1D simulations). Moreover, the quasi-1D results utilize constant specific heat ratios while the 2D results use variable specific heat ratios. As a consequence, even the baseline PDRE results vary between the two simulations, shown in Figure 11. Despite such differences, it is apparent that the quasi-1D PDRIME simulations predict performance enhancement while the 2D simulations do not, as seen in the figure.

The disparity between MHD effects in Figure 11 is largely explained by the significant two-dimensional effects occurring at the contact surface between the bypass outflow and nozzle exhaust. A sample of the 2D time-evolution of temperature for the Mach 9 condition at 25 km, including streamlines, is shown in Figure 12. While the quasi-1D simulation assumes a bypass exit boundary condition consisting of a vertical wall of stagnant, high

pressure fluid, in reality the contact surface between the bypass and nozzle outflows is at a variable angle. The bypass flow travels up the contact surface before circling back along the extended bypass upper wall, creating significant vortical structures that the quasi-1D simulations cannot resolve, leading to different conditions under which the bypass accelerator operates. While the temperature field appears to be roughly one-dimensional in the bypass section, the substantial vorticity generation alters the flow from that assumed in quasi-1D simulations.

E. PDRIME Simulations with Cesium Ionization

We now represent the more realistic effects of the seeding, ionization, deionization, and transport of cesium in the nozzle and bypass in the 2D simulations and calculate the conductivity directly to see how this influences performance. The initial conditions, flight conditions, magnetic field strengths, and PDRIME dimensions are the same. To the chamber we add a mixture of cesium atoms and ions at equilibrium, amounting to 0.5% of chamber's initial contents on a molar basis. We assume the converging section of the nozzle to be short enough that the level of deionization occuring between the chamber and the nozzle to be negligible. To the bypass inlet, we add 0.1% cesium atoms on a molar basis.

PDRE simulations of cesium ionization with the nozzle generator active can produce conductivity in the nozzle at 1000 Mho/m, as prescribed in the simplified simulations, but only if the initial chamber temperature is set to 4000 K rather than 3000 K. Thus, for this next set of simulations, only a 4000 K chamber pressure initialization will be utilized. Matching conductivity levels for the 3000 K initialization would require increasing increasing the molar percentage of cesium in the nozzle inlet to 2% of the fluid by moles, or 14% by mass, which would be excessive.

Running similar test cases as before, with results in Figure 13, reveals that we are once again unable to obtain significant impulse improvements over the baseline total of 1000 N-s per cycle. Variances between the results in Figure 9 and those in Figure 13 arise from the fact that the nozzle fluid conductivity profiles in the former are constant at 1000 Mho/m while those in the latter are transient, despite staying near 1000 Mho/m for the majority of the cycle. Furthermore, while the bypass fluid conductivity had previously been assumed to hold constant at 500 Mho/m, results with cesium ionization result in conductivities within the bypass varying between 500 and 2500 Mho/m.

F. Optimization of Engine Operation

In the foregoing PDRIME configuration, the bypass accelerator is able to utilize only a small fraction of the energy provided by the nozzle generator, per the results shown in Figure 8.

In order to prevent unnecessary drag, the remainder of this energy is sent to the chamber piston for consumption, e.g. as in Figure 9, but this not only introduces significant impulse losses (due to alteration of nozzle exit conditions) but also hastens the end of the cycle and thus allows even less time for the bypass section to conduct its work.

One solution is to generate less energy in the first place by reducing either the nozzle flow conductivity or the MHD generator magnetic field strength. This approach would result in a reduced nozzle exit pressure, higher exit Mach number, and reduced heating in the bypass section, but here the bypass accelerator would not eject the fluid as quickly as before, and it might be able to consume a greater percent of the total available energy, leaving less for the magnetic piston and lowered impulse losses.

Hence, rather than focus on heating the bypass fluid to as high a temperature as possible, an alternative objective is to provide the bypass with as much ionized, low-velocity fluid as possible, even if the fluid is relatively weakly ionized. The air mass in the bypass can be increased by either reducing the altitude to increase its density or by widening the bypass tube to increase its volume. Both of these methods have the drawback of inhibiting propagation of the nozzle-driven shock upstream in the bypass tube, but this can be compensated by reducing the flight Mach number. All of these changes will result in a weaker shock and thus reduced conductivity, on the order of 300-400 Mho/m in the nozzle and 100-200 Mho/m in the bypass, so ejecting the increased shock will take more time. If the piston is activated too early, it might consume energy that the bypass accelerator would have utilized had the cycle been allowed to run longer. Thus, this change to the PDRIME operating conditions will be to desynchronize the generator from the chamber piston, setting the latter to activate at some time after the former shuts off and allowing more time for the bypass accelerator to function.

The next set of results utilizes all of these suggested improvements at once. The PDRE chamber is initially set to 100 atm and 3000 K, the bypass width is increased to 15 cm, the flight Mach number is reduced to 2, and the altitude is reduced to 20 atm so that the bypass inlet pressure and temperature are 5529 Pa and 216 K, respectively. The bypass accelerator continues to run with a uniform magnetic field of 3T and activates only on fluids that travel slower than 1000 m/s and temperatures above 300K so that the simulation does not mistake the trace ionization in the unheated bypass fluid as viable ejection material. The bypass length remains at 3 m, and the nozzle dimensions remain the same as in previous tests.

The results in Figure 14 show that this new PDRIME configuration is much more effective than prior configurations. In contrast to the baseline PDRE (but with cesium seeding to replicate PDRIME mass addition), the PDRIME with the bypass alone has an increase in cycle impulse of 80 N-s, and since the chamber piston utilizes very little energy, it also costs very little in impulse losses, netting the PDRIME a 65 N-s impulse improvement over the

baseline. Figure 15 illustrates how the energy consumption by the magnetic piston and the bypass accelerator is slow and steady, occurring right up until the end of the cycle at roughly 0.012 seconds.

We run similar tests for a variety of flight Mach numbers and bypass widths, in all of which the generator shuts off when the chamber pressure reaches 30 atm. The time at which the piston activates varies according to that which produces the most efficient performance under the flight conditions. In these cases, the chamber pressure at which the piston activates lies between 8 atm for the lower flight Mach numbers and 18 atm for the higher Mach numbers. Figure 16 demonstrates that for these calculations, there is increasing impulse improvement with a reduced flight Mach number. At lower Mach numbers, increasing the bypass width also increases performance by facilitating the ionization of additional fluid, but as the flight Mach number increases, increasing bypass width produces diminishing returns as the extra inlet mass starts expelling the upstream shock before the bypass accelerator has a chance to operate effectively on the ionized gas. Less energy is redirected into the bypass flow this way, thus necessitating earlier chamber piston activation to make certain that all stored energy is reintroduced. Accounting for cesium seeding in the baseline and PDRIME configurations, Figure 16 shows up to a 70 N-s increase in impulse for Mach 2 operation.

Running the same experiments at altitudes of 25 km and 30 km requires an adjustment to the PDRIME, since in some cases the reduced inlet bypass pressure results in the upstream shock's escaping the tube and taking useful heat energy with it. Thus, at 25 km and 30 km, we run the same tests with a bypass of length 4 meters and 6 meters, respectively. Figures 17 and 18 illustrate how we are able to obtain similar results at these altitudes as we did at 20 km (Figure 16) for the same ranges of flight Mach numbers and bypass widths. In these cases, the shock waves propogate further up the bypass tube and heat the air to higher temperatures, but these are compensated by the reduced air density and greater distances over which the fluid must be accelerated.

Despite the similar impulse results per cycle, one significant drawback to operating at higher altitudes is that longer bypass tubes are required to accelerate the extra volume of less dense air, necessitating a heavier PDRIME device with additional electromagnetic components such as magnets. Bypass lengths in excess of 3 meters are not required for the higher flight Mach numbers tested, but the best impulse improvement is observed at the lowest flight Mach numbers, thereby rendering 20 km to be the optimal altitude at which to operate this PDRIME configuration.

IV. Conclusion

A range of alternative PDRIME configurations and operating conditions have been explored in the present studies. We observe that performance enhancement under the given simulations conditions can be accomplished mainly by the bypass accelerator, and even then only under the condition that it be prevented from accelerating fluid that is already above a given velocity. While the magnetic chamber piston can be utilized early in the cycle to maintain higher nozzle exit pressure and can aid in causing the shock to propagate up the bypass tube, the piston can also hasten the end of the cycle too quickly for the accelerator to completely eject the heated fluid. This suggests that the piston should be activated later, only as a measure of consuming any energy that would otherwise go unutilized.

The primary method of performance improvement observed in this study is configuring the PDRIME to heat and ionize a large mass of low-velocity bypass flow just enough for the accelerator to efficiently reintroduce as much available energy as possible before the end of the cycle. This configuration is observed to function most efficiently at low flight Mach numbers and at low altitudes, where the inlet air is slow enough to be efficiently accelerated and dense enough to consume sufficient amounts of energy during acceleration. Improved performance can also be observed at higher altitudes, provided that the bypass tube is extended to prevent the nozzle-driven shock from escaping, but the additional weight of the tube and of the electromagnetic components affixed to it would increase the performance requirements of the PDRIME.

Further studies into the breadth of application of the PDRIME could include alternate chamber and nozzle configurations and determining the corresponding optimal operating and flight conditions. Although the present studies were conducted with a low magnetic Reynolds number approximation, future computations would have to account for induced fields. Future simulations might also operate the bypass ejector in such a way that its cycle period is much longer than that of the chamber detonations, a configuration which cannot be simulated using only the blowdown model, as done in the present studies. All of these simulations eventually require full coupling of the electric and magnetic fields as well as more detailed analysis of cesium ionization, beyond a single reversible reaction, to determine the complete feasibility.

Acknowledgments

The authors wish to acknowledge the technical assistance of Dr. Xing He of HyperComp, Inc. in the early stages of this work. This research has been supported at UCLA by the Air Force Office of Scientific Research under the space power and propulsion program managed

by Dr. Mitat Birkan (Grants FA9550-07-1-0156 and FA9550-07-1-0368).

References

[1]Cambier, J.-L., Roth, T., Zeineh, C., and Karagozian, A. R., "The Pulse Detonation Rocket Induced MHD Ejector (PDRIME) Concept," *Proceedings from the 44th AIAA/ASME/SAE/ASEE Joint Propulsion Conference*, July 2008, Paper AIAA-2008-4688.

[2]Zeineh, C., *Numerical Simulation of Magnetohydrodynamic Thrust Augmentation for Pulse Detonation Rocket Engine*, Ph.D. thesis, UCLA Department of Mechanical and Aerospace Engineering, 2010.

[3]Hill, P. and Peterson, C., *Mechanics and Thermodynamics of Propulsion*, Addison-Wesley publishing company, 2nd ed., 1992.

[4]Eidelman, S., Grossmann, W., and Lottati, I., "Review of Propulsion Applications and Numerical Simulations of the Pulse Detonation Engine Concept," *Journal of Propulsion and Power*, Vol. 7, No. 6, 1991, pp. 857–865.

[5]Kailasanath, K. and Patnaik, G., "Performance Estimates of Pulse Detonation Engines," *Proceedings of the Combustion Institute*, Vol. 28, 2000, pp. 595–602.

[6]Cooper, M. and Shepherd, J. E., "Single Cycle Impulse from Detonation Tubes with Nozzles," *Journal of Propulsion and Power*, Vol. 24, No. 1, 2008, pp. 81–87.

[7]Wintenberger, E., Austin, J. M., Cooper, M., Jackson, S., and Shepherd, J. E., "An Analytical Model for the Impulse of a Single Cycle Pulse Detonation Engine," *Journal of Propulsion and Power*, Vol. 19, No. 4, 2003, pp. 22–38, also Journal of Propulsion and Power, Vol. 20, No. 4, 2004, pp. 765–767.

[8]Li, C. and Kailasanath, K., "Partial Fuel Filling in Pulse Detonation Engines," *Journal of Propulsion and Power*, Vol. 19, No. 5, 2003, pp. 908–916.

[9]Warwick, G., "U.S. AFRL proves pulse-detonation engine can power aircraft," *Flight Magazine*, March 5 2008, (online at http://www.flightglobal.com/articles/2008/03/05/222008/us-afrl-proves-pulse-detonation-engine-can-power-aircraft.html).

[10]He, X. and Karagozian, A. R., "Numerical Simulation of Pulse Detonation Engine Phenomena," *Journal of Scientific Computing*, Vol. 19, No. 1–3, Dec. 2003, pp. 201–224.

[11]He, X. and Karagozian, A. R., "Pulse Detonation Engine Simulations with Alternative Geometries and Reaction Kinetics," *Journal of Propulsion and Power*, Vol. 22, No. 4, 2006, pp. 852–861.

[12]Harten, A., Osher, S. J., Engquist, B. E., and Chakravarthy, S. R., "Some Results on Uniformly High-Order Accurate Essentially Nonoscillatory Schemes," *Journal of Applied Numerical Math*, Vol. 2, 1986, pp. 347–377.

[13]Jiang, G. S. and Shu, C. W., "Efficient Implementation of Weighted ENO Schemes," *Journal of Computational Physics*, Vol. 126, 1996, pp. 202–228.

[14]Cambier, J.-L., "MHD Augmentation of Pulse Detonation Rocket Engines," *Proceedings from the 10th Intl. Space Planes Conf.*, Kyoto, Japan, April 2001, AIAA paper 2001-1782.

[15]O'Sullivan, M. N., Krasnodebski, J. K., Waitz, I. A., Gretizer, E. M., and Tan, C. S., "Computational Study of Viscous Effects on Lobed Mixer Flow Features and Performance," *Journal of Propulsion and Power*, Vol. 12, No. 3, 1996, pp. 449–456.

[16]Cambier, J.-L., "A Thermodynamic Study of MHD Ejectors," *Proceedings from the 34th AIAA/ASME/SAE/ASEE Joint Propulsion Conference*, July 1998, AIAA paper 1998-2827.

[17]Hwang, P., Fedkiw, R. P., Merriman, B., Aslam, T. D., Karagozian, A. R., and Osher, S. J., "Numerical Resolution of Pulsating Detonation Waves," *Combustion Theory and Modelling*, Vol. 4, No. 3, Sept. 2000, pp. 217–240.

[18]Henrick, A. K., Aslam, T. D., and Powers, J. M., "Mapped Weighted Essentially Non-oscillatory Schemes: Achieving Optimal Order near Critical Points," *Journal of Computational Physics*, Vol. 207, No. 2, 2005, pp. 542–567.

[19]Cambier, J.-L., "Preliminary Model of Pulse Detonation Rocket Engines," *Proceedings from the 35th AIAA/ASME/SAE/ASEE Joint Propulsion Conference*, June 1999, AIAA paper 1999-2659.

[20]Roth, T., *Modeling and Numerical Simulations of Pulse Detonation Engines with MHD Thrust Augmentation*, Master's thesis, Department of Mechanical and Aerospace Engineering, UCLA, 2007.

[21]Cole, L., "Combustion and magnetohydrodynamic processes in advanced pulse detonation rocket engines," 2010, Ph.D. prospectus, Department of Mechanical and Aerospace Engineering, UCLA.

A_{cham}	A^*	A_e	A_{byp}	L_{cham}	L_{conv}	L_{div}	L_{byp}	L_{uwall}	L_{open}
0.1256	0.02513	0.06283	0.06	0.50	0.02	0.80	3.00	0.40	1.60

Table 1. Dimensions of the PDRIME in meters and meters^2 for lengths and areas, respectively.

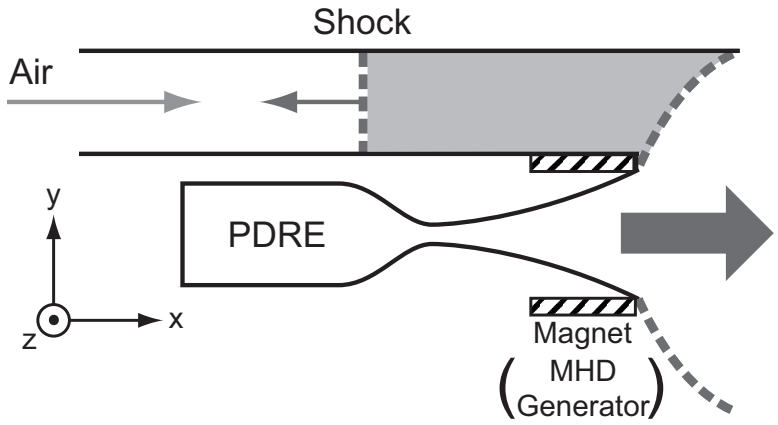

Figure 1a. Schematic of the PDRIME concept during the initial portion of the cycle. Overpressure at the nozzle exit allows an upstream propagating shock (dashed line) to enter the bypass section. This shock slows and raises the temperature of the seeded air in the bypass channel, shown in the shaded portion of the figure. A magnet adjacent to the nozzle extracts energy from the flow.

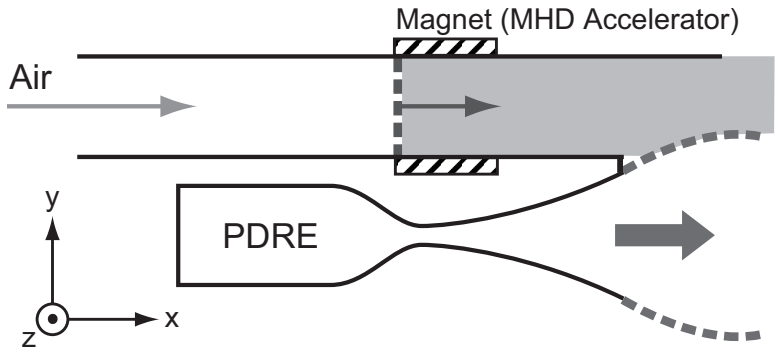

Figure 1b. Schematic of the PDRIME concept in the latter part of the cycle, during blowdown. As the pressure at the nozzle exit drops, exhaust of the compressed and heated air from the bypass channel takes place. Power is applied via the magnets shown, resulting in the MHD acceleration of the air slug in the bypass channel.

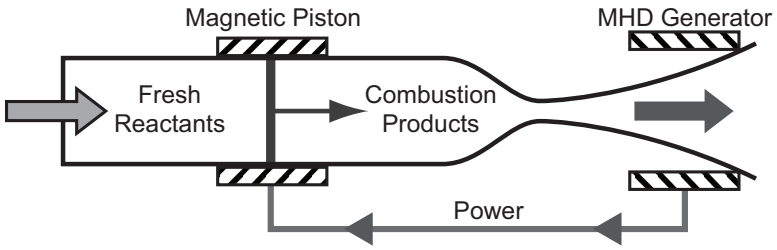

Figure 2. Schematic of the Magnetic Piston Concept. The piston accelerates the combustion products out of the chamber in such a way that, as long as it continuously operates, constant pressure and temperature are maintained at the throat. Fresh reactants are simulatenously drawn in to replace the evacuated products.

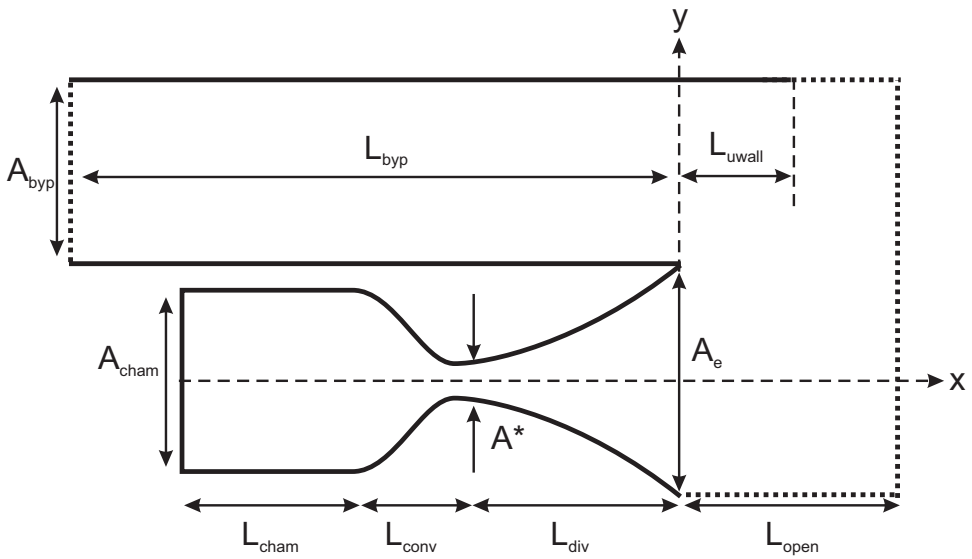

Figure 3. General configuration of a planar PDRIME of unit depth. The parabolic contour of the nozzle wall and the extension of the upper bypass wall assist in the transfer of high-pressure products from the nozzle exit to the bypass exit.

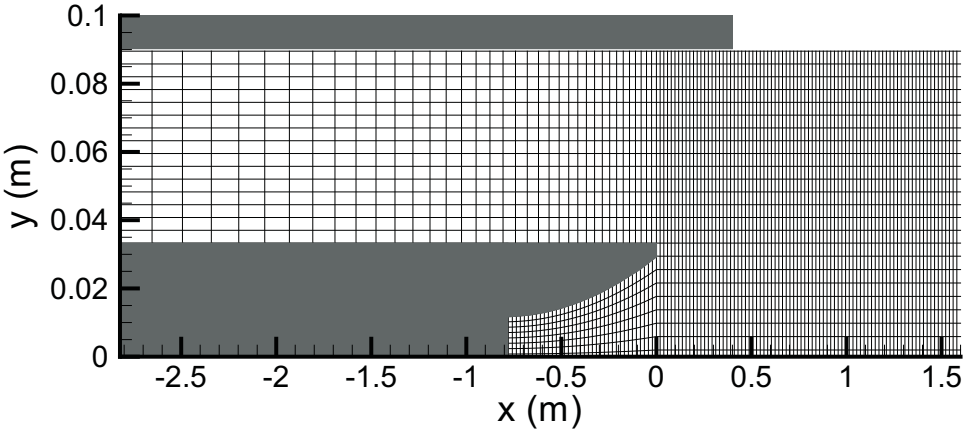

Figure 4. Two-dimensional planar PDRIME domain of real cells.

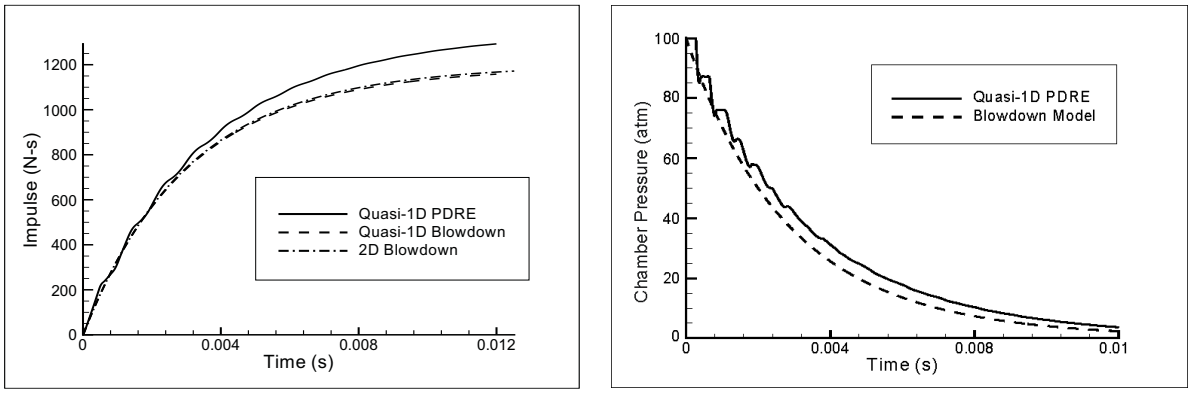

(a) Total Impulse (N-s) (b) Chamber Pressure (atm)

Figure 5. Comparisons among the quasi-1D PDRE simulation, the quasi-1D blowdown nozzle simulation, and the 2D blowdown nozzle simulation. (a) shows impulse and (b) shows chamber pressure as a function of time. The chamber pressure blowdown model in (b) is identical in both quasi-1D and 2D simulations.

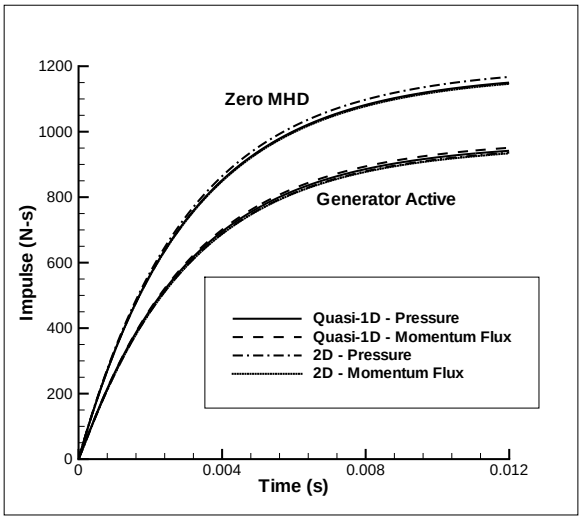

Figure 6. Impulse calculation test comparing quasi-1D and 2D simulations of a PDRE with an area ratio AR=2.5. The pressure- and momentum-based methods employ wall pressure and momentum flux integrations. Results with and without the MHD generator active in the nozzle are shown, for both quasi-1D and 2D simulations.

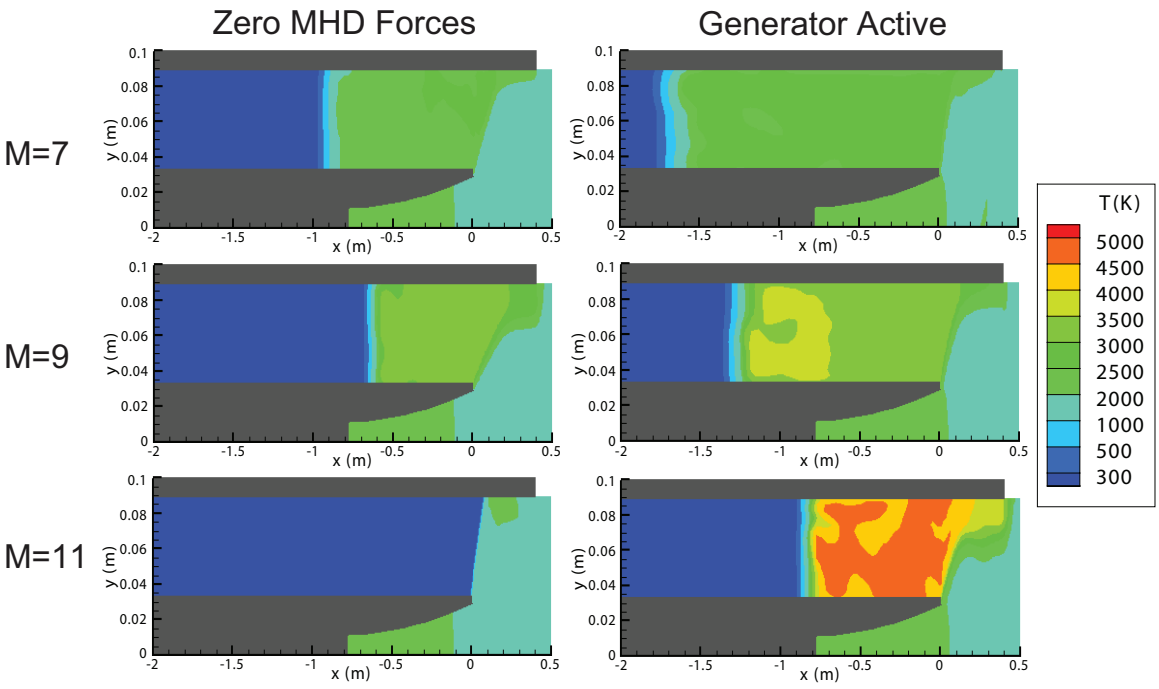

Figure 7. Temperature contours of the PDRIME, with and without the nozzle generator running, at time t=3ms. The altitude of operation is 25 km, with an initial chamber temperature of 3000 K.

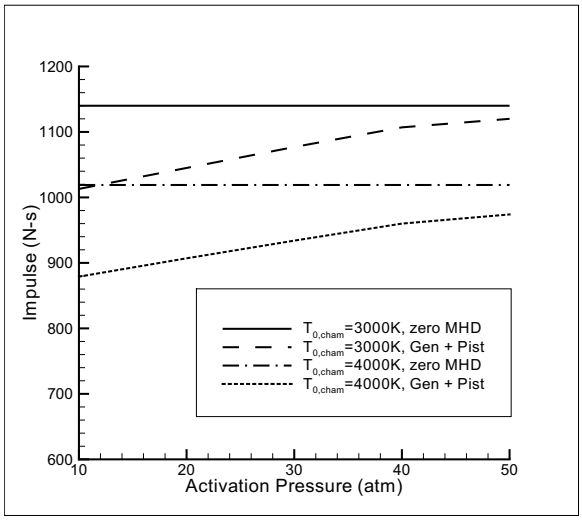

(a) Shutdown/Activation Pressure Test - Impulse

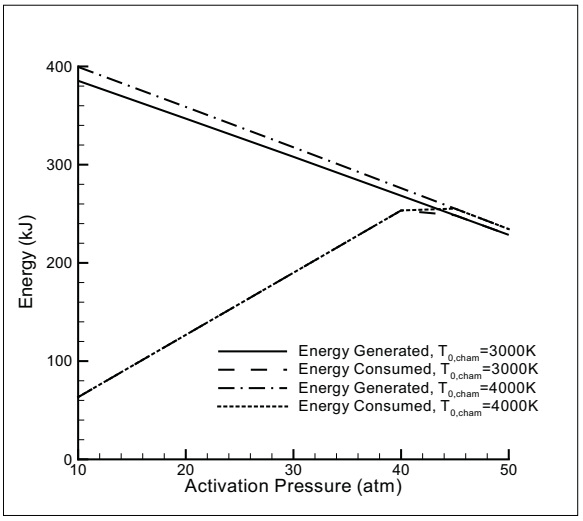

(b) Shutdown/Activation Pressure Test - Energy

Figure 8. PDRE operation utilizing the MHD generator in series with the magnetic chamber piston. The MHD generator operates from the beginning of the cycle, and the time at which the generator deactivates and the piston activates is determined by the chamber activation pressure. Lower activation pressures result in the generator running for longer periods of time, producing more energy than the piston can consume before expelling all remaining products. Higher activation pressures result in the generator running for shorter periods of time, producing less energy, all of which can be utilized by the piston in the same cycle. Simulations are run for initial chamber temperatures of 3000 K and 4000 K.

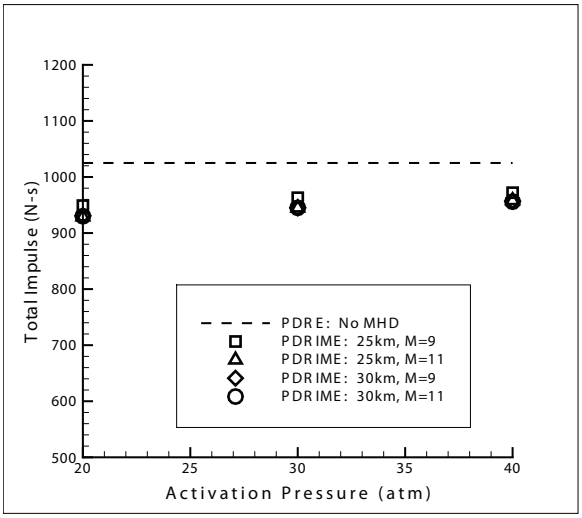

Figure 9. Total impulse for several constant-conductivity PDRE simulations in which initial chamber temperature is set to 4000 K. The dashed line indicates the minimum impulse that the bypass must contribute in order to outperform the PDRE without any MHD components.

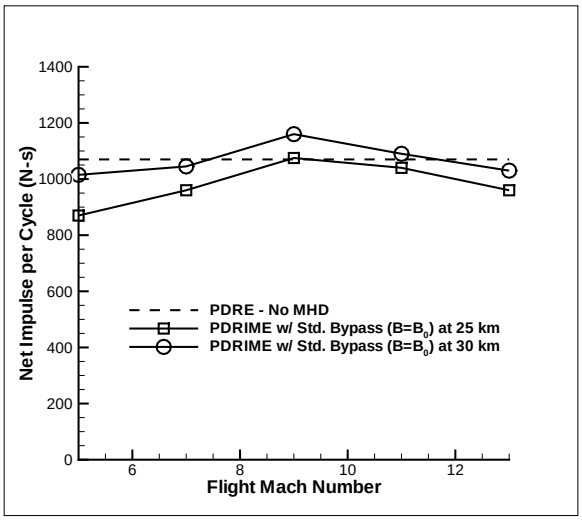

Figure 10. Total impulse for quasi-1D, constant-conductivity PDRIME simulations in which initial chamber temperature is set to 3000 K. The dashed line indicates the minimum impulse that the bypass must contribute in order to outperform the PDRE without any MHD components.

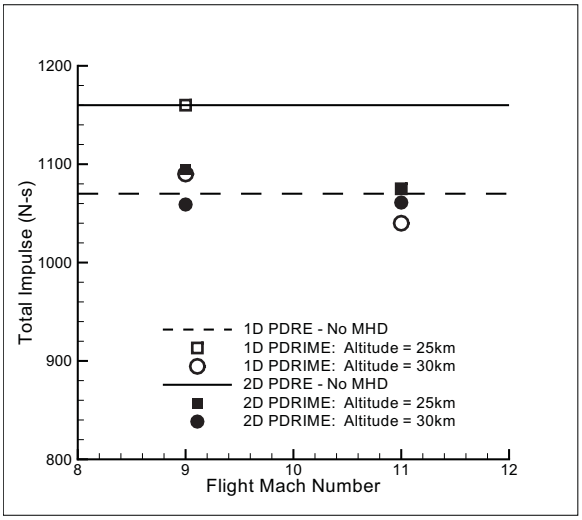

Figure 11. Comparisons between quasi-1D and 2D simulations of the PDRIME in which initial chamber temperature is set to 3000 K and conductivity is constant. The dashed and solid lines indicate the minimum impulse that the bypass must contribute in order to outperform the PDRE without any MHD components for the quasi-1D and 2D simulations, respectively.

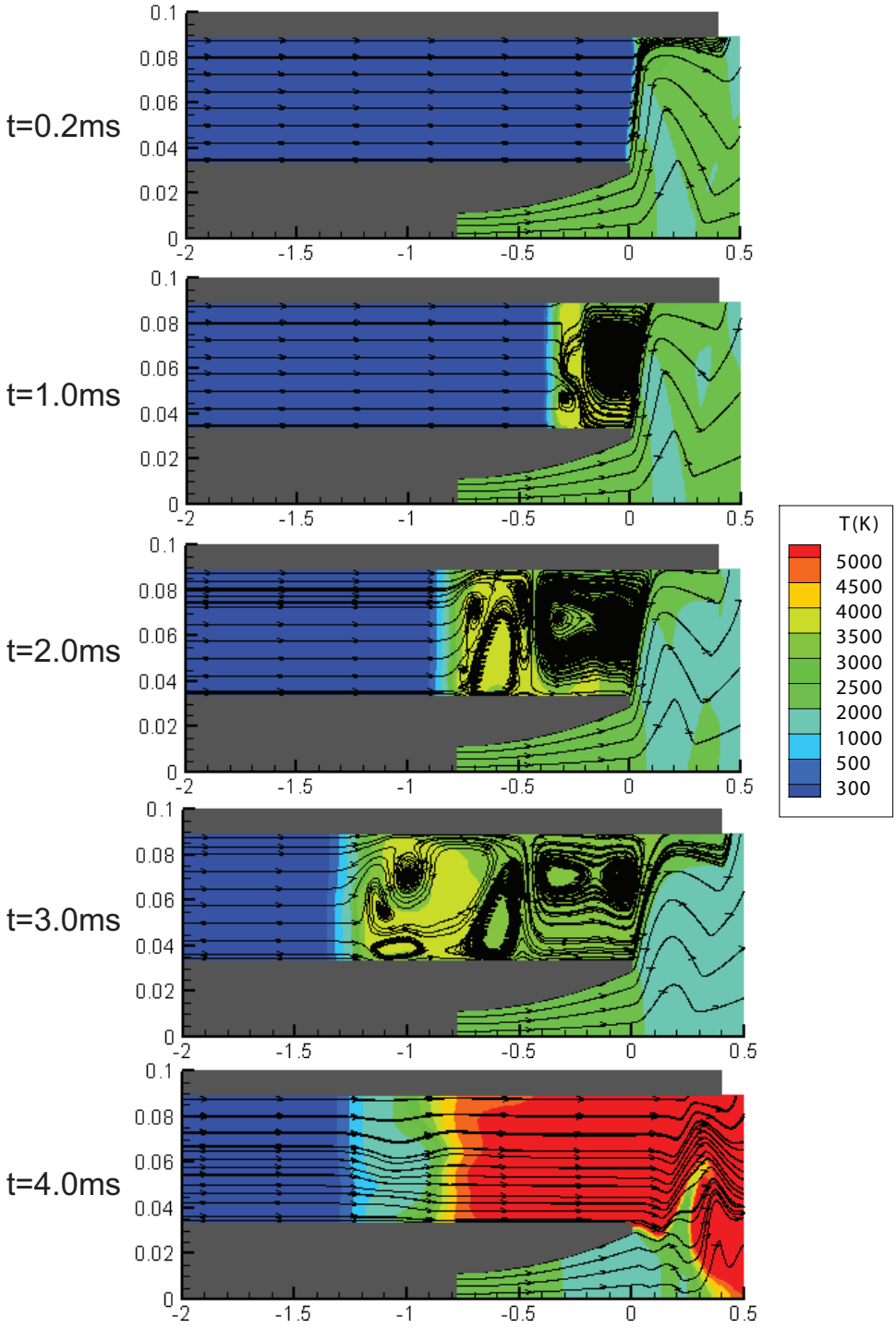

Figure 12. Temperature contours of the PDRIME with the nozzle generator, superimposed with streamlines to illustrate fragmented vortical structures. The altitude is 25 km, the initial chamber temperature is 3000 K, and the Mach number is 9.

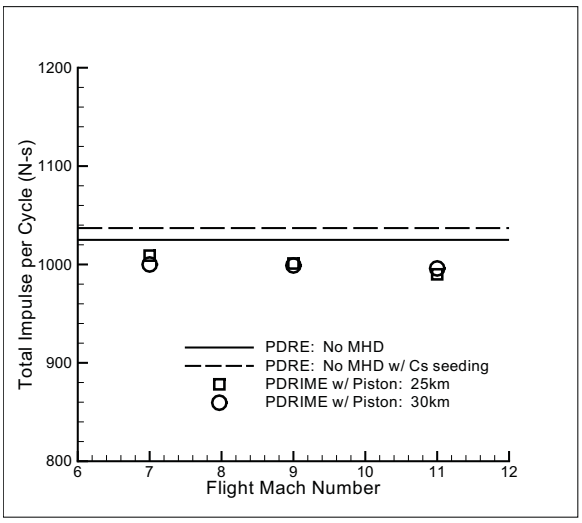

Figure 13. Maximum total impulse for several 2D simulations with cesium ionization and deionization. The chamber temperature is initialized to 4000 K. The solid line indicates the total impulse of the PDRE without any MHD components or seeding of cesium. The dashed line indicates the total PDRE impulse with no MHD components but with the additional mass of cesium added. The dashed line indicates the minimum impulse that the bypass must contribute in order to outperform the PDRE without any MHD components.

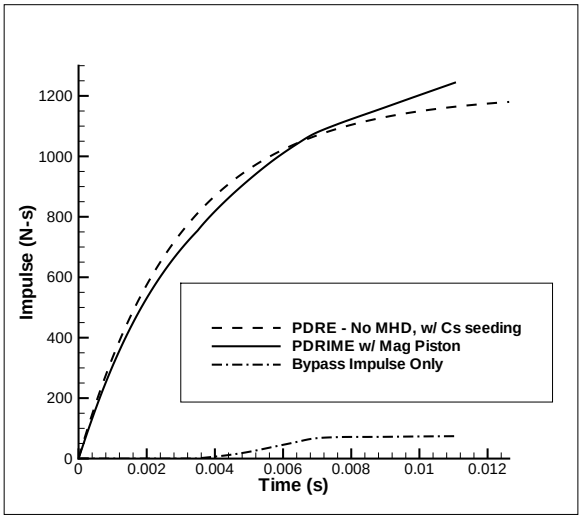

Figure 14. PDRIME performance at 20km and flight Mach 2 with initial chamber temperature of 3000 K. Impulse evolution is plotted for both a baseline PDRE seeded with cesium but with no MHD activation and a PDRIME with the nozzle generator, bypass accelerator, and chamber piston actiavted. An additional impulse plot illustrates the contribution from the bypass accelerator during the PDRIME simulation. Chamber-to-throat area ratio = 5.0, exit-to-throat AR=2.5, bypass width = 15 cm. Chamber is initially seeded with 0.5% cesium by moles, and the width of the bypass is seeded with 0.1% cesium by moles. The accelerator limit is set to 1000 m/s.

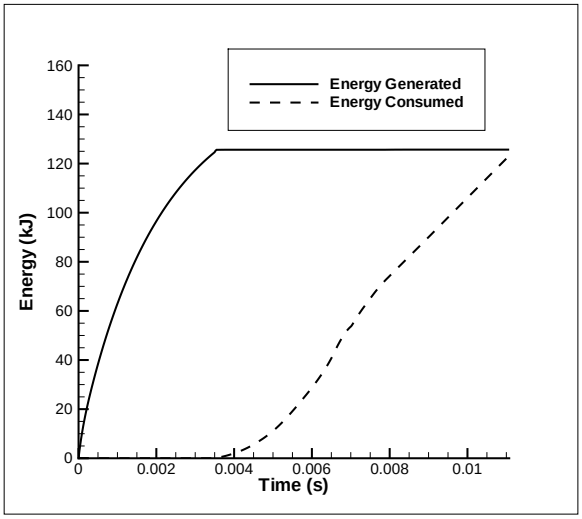

Figure 15. PDRIME energy generation and consumption at 20km and flight Mach 2 with initial chamber temperature of 3000 K. The solid line illustrates the initial activation of the nozzle generator and its shutoff at roughly 0.0035 second. At this time, the dashed line illustrates the chamber piston activating, followed by a gradual consumption of energy from the bypass accelerator. Chamber-to-throat area ratio = 5.0, exit-to-throat AR=2.5. Bypass width = 15 cm. Chamber is initially seeded with 0.5% cesium by moles, and the width of the bypass is seeded with 0.1% cesium by moles. The accelerator limit is set to 1000 m/s.

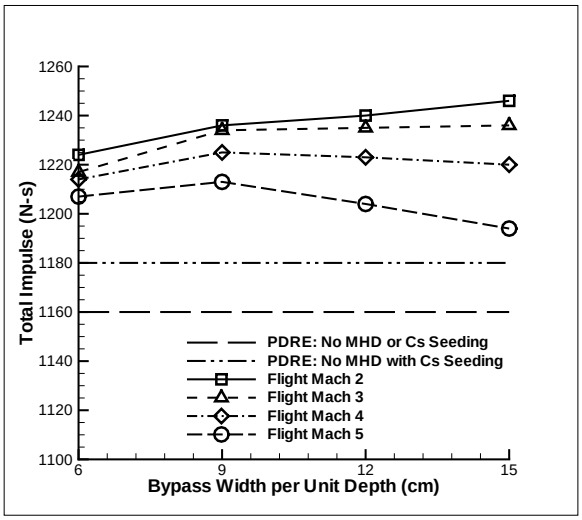

Figure 16. PDRIME total impulse per cycle at 20km varying with flight Mach number and bypass area per unit depth. Initial chamber temperature of 3000 K. Bypass length = 3 m. Chamber is initially seeded with 0.5% cesium by moles, and the width of the bypass is seeded with 0.1% cesium by moles. The accelerator limit is set to 1000 m/s.

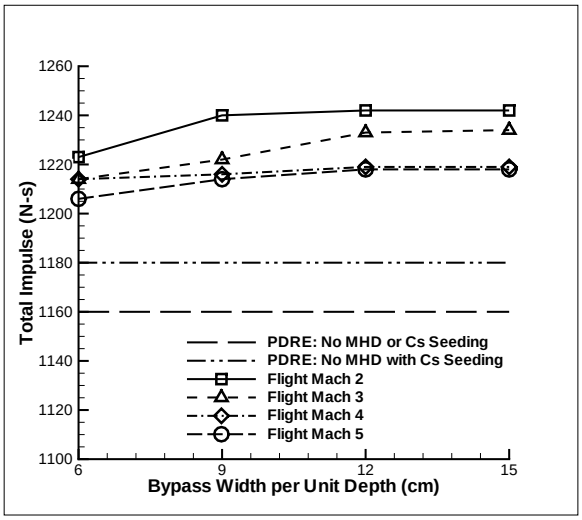

Figure 17. PDRIME total impulse per cycle at 25km varying with flight Mach number and bypass area per unit depth. Initial chamber temperature of 3000K. Bypass length = 4m. Chamber is initially seeded with 0.5% cesium by moles, and the width of the bypass is seeded with 0.1% cesium by moles. The accelerator limit is set to 1000 m/s.

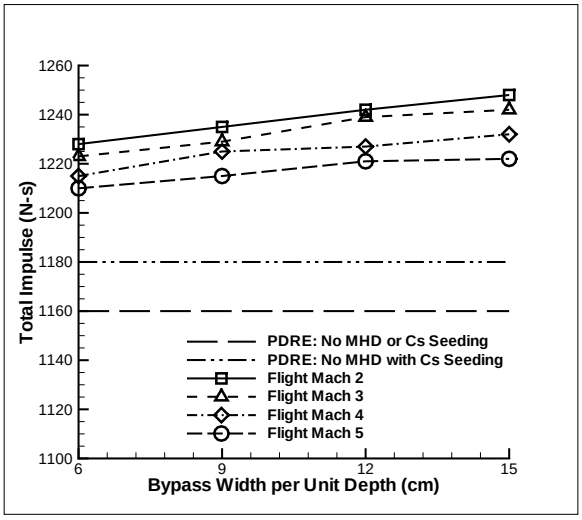

Figure 18. PDRIME total impulse per cycle at 30km varying with flight Mach number and bypass area per unit depth. Initial chamber temperature of 3000K. Bypass length = 6m. Chamber is initially seeded with 0.5% cesium by moles, and the width of the bypass is seeded with 0.1% cesium by moles. Accelerator limit set to 1000 m/s.